NRC Publications Archive
Archives des publications du CNRC

Load path optimization in tube hydroforming

Mojarad, S.; Champliaud, H.; Gholipour, J.; Savoie, J.; Wanjara, P.

This publication could be one of several versions: author's original, accepted manuscript or the publisher's version. / La version de cette publication peut être l'une des suivantes : la version prépublication de l'auteur, la version acceptée du manuscrit ou la version de l'éditeur.
For the publisher's version, please access the DOI link below./ Pour consulter la version de l'éditeur, utilisez le lien DOI ci-dessous.

Publisher's version / Version de l'éditeur:
https://doi.org/10.5589/q15-003
Canadian Aeronautics and Space Journal, 60, 3, pp. 82-89, 2015-03-02

NRC Publications Record / Notice d'Archives des publications de CNRC:
https://nrc-publications.canada.ca/eng/view/object/?id=f44b7f44-972e-4b51-a441-9a665503161b
https://publications-cnrc.canada.ca/fra/voir/objet/?id=f44b7f44-972e-4b51-a441-9a665503161b

Access and use of this website and the material on it are subject to the Terms and Conditions set forth at
https://nrc-publications.canada.ca/eng/copyright
READ THESE TERMS AND CONDITIONS CAREFULLY BEFORE USING THIS WEBSITE.

L'accès à ce site Web et l'utilisation de son contenu sont assujettis aux conditions présentées dans le site
https://publications-cnrc.canada.ca/fra/droits
LISEZ CES CONDITIONS ATTENTIVEMENT AVANT D'UTILISER CE SITE WEB.

Questions? Contact the NRC Publications Archive team at PublicationsArchive-ArchivesPublications@nrc-cnrc.gc.ca. If you wish to email the authors directly, please see the first page of the publication for their contact information.

Vous avez des questions? Nous pouvons vous aider. Pour communiquer directement avec un auteur, consultez la première page de la revue dans laquelle son article a été publié afin de trouver ses coordonnées. Si vous n'arrivez pas à les repérer, communiquez avec nous à PublicationsArchive-ArchivesPublications@nrc-cnrc.gc.ca.

National Research Council Canada
Conseil national de recherches Canada
Canada

Can. Aeronaut. Space J., Vol. 60, No. 3, pp. 82–89, 2014

Load path optimization in tube hydroforming

S. Mojarad, H. Champliaud, J. Gholipour, J. Savoie, and P. Wanjara

Abstract. The goal of this work was to identify the optimum combination of the main process parameters, i.e., the internal pressure and end feeding (load path), for tube hydroforming to minimize the thickness reduction, while satisfying the failure constraint defined by the forming limit diagram of the material. To perform process design optimization with minimum experimentation, the LS-OPT software was utilized in combination with a finite element model (FEM) that simulated a round to square tube hydroforming (THF) process for stainless steel 321 in LS-DYNA. The load path obtained through the optimization procedure was applied to the THF process and the tube expansion and the thickness results obtained from the FEM were compared with the experimental results in the critical regions of the hydroformed tube.

Résumé. L'objectif de cette étude était de déterminer la combinaison optimale des principaux paramètres du procédé, c'est-à-dire la pression interne et la compression axiale (chemin de chargement) pour l'hydroformage des tubes afin de minimiser la réduction de l'épaisseur, tout en satisfaisant la contrainte de rupture définie par le Courbes limite de formage de la matière. Pour effectuer l'optimisation de la conception du procédé avec un minimum d'expérimentation, le logiciel LS-OPT a été utilisé en combinaison avec un modèle par éléments finis (MEF) qui a simulé le procédé d'hydroformage de tubes (HFT) de forme ronde à carrée appliqué à l'acier inoxydable 321 à partir du logiciel LS-DYNA. Le chemin de chargement obtenu par la procédure d'optimisation a été appliqué au procédé HFT et l'expansion de tube et les résultats d'épaisseur obtenus à partir du MEF ont été comparés avec les résultats expérimentaux dans les zones critiques du tube hydroformé. [Traduit par la Rédaction]

Can. Aeronaut. Space J. Downloaded from pubs.casi.ca by April Duffy on 07/14/15
For personal use only.

Introduction

Many parameters are involved in the tube hydroforming (THF) process, such as the formability of the material, load path (combination of end feeding and internal pressure), tool geometry, and friction. Through a good understanding of these parameters, the process can be designed and controlled to improve the quality, performance, and reliability of the final product. Among the different process parameters, load path is the most important in THF. Traditionally, determination of the load path in THF has relied on a trial and error procedure (Fann and Hsiao, 2003), which was time consuming, and yet remained nonsystematic and did not assure an optimum load path. The effectiveness of trial and error experimentation decreased, especially when designing the manufacturing process with new materials and (or) die geometries, for which no prior knowledge was available. For this reason, more recently, finite element analysis (FEA) is more widely used as a powerful tool for analyzing the effects of different process parameters on THF of complex geometries (Gholipour et al., 2004). Hama et al. (2006) developed a finite element model (FEM) to simulate the effects of three different load paths, namely pressure advanced, linear, and feed advanced, for THF of a part with a rectangular cross section. The results showed that the pressure-advanced load path, in which the internal pressure increases to a threshold value prior to starting the axial end feeding, leads to a higher formability as the initial internal pressure prevents local wrinkling in the early stages of the process. In contrast, for an X-shape geometry, Ray and MacDonald (2005) recommended using a feed-advanced load path, as the pressure-advanced load path could cause premature bursting during THF due to excessive wall thinning at the critical regions. Clearly, there may be numerous possible load paths for THF of a given geometry; however, finding the optimum load path remains a predominant challenge for manufacturing that can be addressed cost efficiently and effectively through an optimization tool.

There are two main approaches for optimizing load path in the THF process, namely, the adaptive simulation method and optimization procedures (Jansson et al., 2007). In the adaptive method, the finite element simulation is continuously monitored for defects such as wrinkling or excessive thinning, and the input values for the parameters are adjusted accordingly in the subsequent iteration until a solution is attained. This procedure has been used by many researchers to optimize the load path in THF (Aydemir et al., 2005; Johnson et al., 2004; Labergere and Gelin, 2004; Ray and Mac Donald, 2004; Mataei et al., 2011) as it has the advantage of providing the optimum process parameters through simulating a single FEM. Alternatively, for the

Received 2 June 2014. Accepted 17 September 2014. Published on the Web at http://pubs.casi.ca/journal/casj on 2 March 2015.

S. Mojarad and H. Champliaud. Department of Mechanical Engineering, École de technologie supérieure, Montréal, Canada.

J. Gholipour* and P. Wanjara. National Research Council Canada, Aerospace, Montréal, Canada.

J. Savoie. Pratt & Whitney Canada, Special Process Development Group, Longueuil, Canada.

*Corresponding author (e-mail: Javad.GholipourBaradari@cnrc-nrc.gc.ca)

© 2015 Government of Canada

Can. Aeronaut. Space J. Downloaded from pubs.casi.ca by April Duffy on 07/14/15
For personal use only.

other approach, i.e., optimization procedures, the optimum solution is attained by repeating multiple simulations of the FEM through iterations within the defined constraints of the process. In general, the optimization procedures are divided into three sub-groups including iterative algorithms, genetic algorithms, and approximate optimization algorithms (Meinders et al., 2008). The iterative optimization algorithms, for instance the conjugate gradient method, converge to an optimum solution based on minimizing an objective function through repeated simulations of the FEM. Though these well-known algorithms are widely applied to optimize the THF process parameters (Endelt and Nielsen, 2001; Fann and Hsiao, 2003; Jirathearanat and Altan, 2004; Sillekens and Werkhoven, 2001; Yang et al., 2001), their main disadvantage is a tendency to become trapped in finding local minima instead of global solutions. To overcome this disadvantage, genetic algorithms, which are optimizing methods that mimic the process of natural evolution, have been used to find the global optimum solution. Specifically, in the genetic algorithm, the values of the process parameters that lead to the optimum result are selected as inputs for the next iteration of the FEM simulation. For instance, Abedrabbo et al. (2011) utilized this method with LS-DYNA to optimize the load path in a THF process. However, a main drawback of such genetic algorithms is the large number of required simulations, and thus the relatively long processing time needed to obtain a global solution. As such, optimization algorithms, of which a well-known method is the response surface methodology (RSM), have been considered over evolutionary algorithms for metal forming processes (Alaswad et al., 2010; Koç et al., 2000) to find the global optimum solution due to their shorter processing times. In particular, in the RSM, a set of input values for the process parameters are selected and, through simulations of the FEM, the response of each set is calculated. Then a low order polynomial is used to fit the response points, and the best combination of input values for the parameters is extracted for the next iteration. By repeating this process, the optimized combination can be obtained. To this end, in the current work, the optimum load path for a round to square THF process was studied using a RSM optimization algorithm within LS-OPT in conjunction with LS-DYNA 971 R7. Specifically, the THF process was optimized for stainless steel 321 (SS321) with two different tube thicknesses, initially 0.9 mm and 1.2 mm. For each tube thickness, a FEM was developed for the process, and the optimum load path, determined through the simulations, was validated through experimentation.

Finite element model

ANSYS 14.5 software was used to generate the mesh required for the FEM of a round-to-square THF process. **Figure 1** shows the model, which consisted of the tube and the rigid die. Due to symmetry in the tube and die, the model was simplified by simulating only one-eighth of the geometry. Symmetry boundary constraints were applied to the nodes on the symmetry planes. A total of 17 599 four-node shell elements were used for meshing the tube with Belytschko–Tsay shell element formulation (LS-Dyna Keyword User's Manual, 2013). To capture the strain

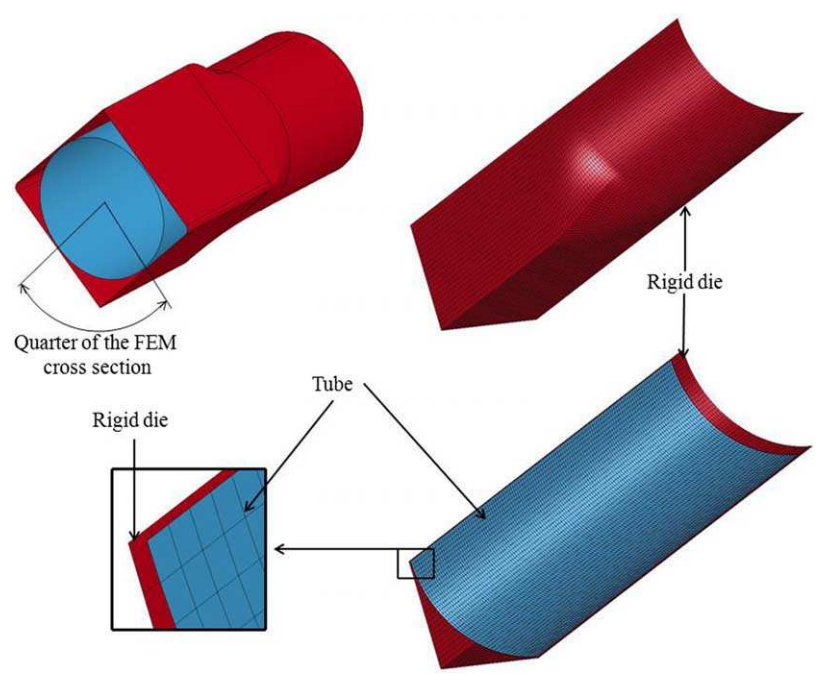

Figure 1. FEM of the round-to-square die.

© 2015 Government of Canada

Can. Aeronaut. Space J. Downloaded from pubs.casi.ca by April Duffy on 07/14/15
For personal use only.

distribution through the thickness, five integration points through the thickness of the tube were considered. As no lubricant was applied to the tubes, a surface to surface contact with a Coulomb coefficient of friction (COF) of 0.2 was used for the contact condition between the tube and the die (Farimani et al., 2013). To simulate end feeding during the process, displacement was assigned to the nodes at the tube end. The Swift work hardening law (Equation (1)) was used to model the material behavior of both tube thicknesses.

$$\sigma = K(\varepsilon_0 + \varepsilon)^n \tag{1}$$

where σ is the true stress, ε is the true strain, ε_0 is the initial true strain, K is the strength coefficient, and n is the strain hardening exponent. The material properties of the 0.9 mm and 1.2 mm thick SS321 tubes were extracted from the free expansion tests. Saboori et al. (2014) developed a semi-analytical online approach that utilizes a 3-D automated deformation measurement system (Aramis®) to measure the coordinates of the bulge profile, the maximum bulge height, and the associated tube thickness to extract the effective stresses and effective strains at different stages of the free expansion process. In this way, bi-axial stress–strain curves for tubular materials can be generated for THF applications. The material parameters for the hardening law were then obtained through a curve fitting procedure based on the least square method. **Table 1** summarizes the material properties used for the tube and the die in the present study.

Optimization

The commercial optimization software, LS_OPT v 4.2, was used to find the optimum load path for the round-to-square THF process. As the objective of the optimization was to minimize the thickness variation in the expansion zone of the hydroformed tubes, the following objective function was defined:

$$\mathrm{Obj} = \left(\frac{\mathrm{MT} - \mathrm{NT}}{\mathrm{NT}}\right)^2 \tag{2}$$

where MT is the minimum tube thickness after hydroforming and NT is the nominal tube thickness before hydroforming. Due to the variation in thickness along the circumferential direction of the initial tube blanks, the average thickness from the measured values was considered in the FEM; the average thickness for the two tube materials considered in this study was 0.94 mm and 1.22 mm. To prevent failure, the forming limit diagram (FLD) for SS321 with a nominal thickness of 0.94 mm and 1.22 mm was calculated based on Hwang's theoretical work (Hwang et al., 2009), in which the FLD was constructed based on free expansion testing, Swift's diffused necking criterion, and Hill's localized necking criterion. Hill's nonquadratic yield function was utilized to derive the critical principal strains at the onset of plastic instability. As such, if the in-plain principal strains in any element of the tube exceed the forming limit curve (FLC), then the applied set of input values would be identified as a failure by the optimization algorithm. **Figure 2** shows the FLCs used for each tube thickness.

Free-end hydroforming, in which no end feeding is applied but the tube ends can move freely during the process, was simulated to find the minimum end feeding that occurs during THF. That is, by increasing the internal pressure, as the tube expands, the material is pulled into the die cavity from both ends of the tube. **Figure 3** illustrates the load path in the free-end hydroforming process for the 0.9 mm and 1.2 mm thick tubes obtained from the FEM. This curve can be used to identify the minimum input values for optimization, which was performed in this work using a single stroke load path approach. It is noteworthy that an end feed value higher than the free-end condition is needed to maintain the seal during the process. Hence, the minimal values (lower band) for the internal pressure and end feeding were selected as 20 MPa and 1.2 mm, respectively. The upper band for the internal pressure was considered to be 100 MPa, which was sufficient for the full expansion of the tube in the THF process. By performing a few simulations of the FEMs, the upper band of end feeding was selected as 20 mm to avoid wrinkling in the tube.

The LS-OPT software required setting of the optimization strategy, sampling method, and algorithm, which were selected as listed in **Table 2**. Specifically, based on the work by An (2010), the strategy was set to be sequential with the domain reduction (SRSM method), which was used by the software for selecting the sampling points in the experimental design. The sampling parameters (i.e., meta-model, order, point-selection, and number of simulation

Table 1. Material properties of the tube (SS321) and the die (Saboori et al., 2014).

Material	SS321 (0.9 mm)	SS321 (1.2 mm)	Die (rigid)
Density (g/mm^3)	8.0E–03	8.0E–03	7.7 E–03
Elastic modulus (MPa)	193.00E + 03	193.00E + 03	2.08E + 06
Poisson ratio	0.29	0.29	0.31
Yielding stress (MPa)	250	260	—
K (MPa)	1427.45	1397.81	—
n	0.53	0.63	—
ε_0	0.03	0.05	—

© 2015 Government of Canada

Can. Aeronaut. Space J. Downloaded from pubs.casi.ca by April Duffy on 07/14/15
For personal use only.

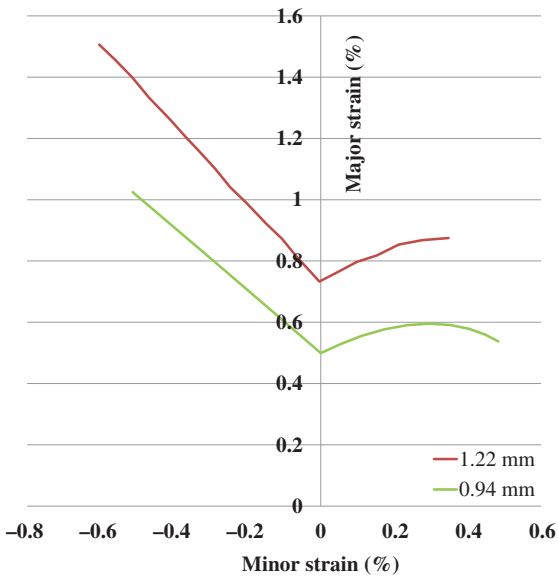

Figure 2. FLD used for the SS321 tubes.

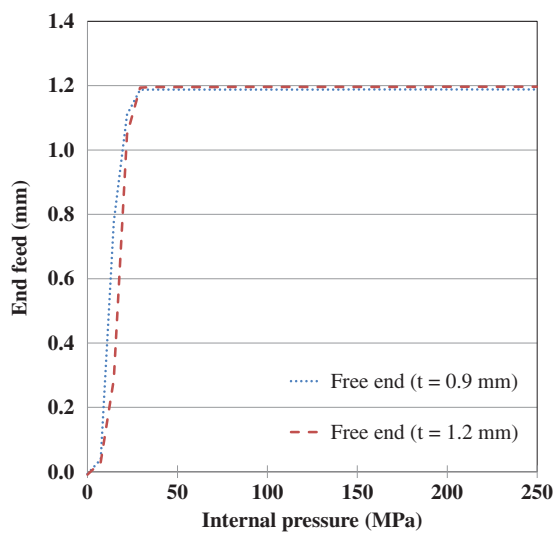

Figure 3. Free-end hydroforming load path from FEA for 0.9 mm and 1.2 mm thick SS321 tubes.

Table 2. Optimization settings in LS-OPT.

Strategy	Sampling parameters	Algorithms
Sequential with domain reduction (SRSM)	(1) Metamodel: polynomial (2) Order: quadratic (3) Point-selection: Doptimal (4) Number of simulation points: 10	Hybrid GA population size: 100 Number of generations: 250

points) related to this strategy were then selected as given **Table 2**. In particular, 10 sampling points for the internal pressure and end feed were selected for each iteration based on Doptimal design (LS-OPT user manual). After the simulation results (responses) for the first iteration, a quadratic polynomial surface (response surface) is passed through the responses. Then a hybrid genetic algorithm (GA) was utilized to find the optimum sampling point of the response surface for the first iteration, and up to 10 iterations were performed to obtain the optimum load path. It is noteworthy that the hybrid GA algorithm starts with the GA to estimate the global optimum solution. Then a gradient-based algorithm is applied to sharpen the solution. With this hybrid method, the computational time was heavily reduced compared with the typical GA method.

Experiments

To verify the FEM results, the THF experiments were conducted at the National Research Council of Canada (NRC) using a fully equipped hydroforming press (**Figure 4**) that was equipped with a round-to-square die set. The die was fabricated from a hardened tool steel and had a square cross section, as illustrated in **Figure 5**. To monitor the expansion of the tubes during the THF process, two laser measurement systems were used in conjunction with two expansion measurement devices on each side of the die. As shown in **Figure 5a**, the distance between the laser measurement system and the expansion measurement device was L_0 at the beginning of the THF process. With the progression of the THF process, the expansion of the tube pushed the pins outward and the distance of the pins (L_n) were recorded sequentially by the laser measurement systems (**Figure 5b**). Hence, the difference between L_n and L_0 is the expansion of the tube at each time increment. It should be noted that the averages of the expansion values obtained from each side (i.e., front and back) are reported in this study.

The THF experiments were conducted on the 0.9 mm and 1.2 mm thick SS321 tubes that had an outer diameter of 50.8 mm and were 220 mm in length. For each tube thickness, the optimum load path, obtained from the optimization process described above, was utilized to hydroform the tubes. **Figure 6** shows the tubes before and after the THF process. For each tube, the thickness at the mid-length cross section after hydroforming was measured using a 38DL Plus Olympus ultrasonic thickness gage device, which is a nondestructive technique. Also, some verification of the thickness evolution was performed in this work through sectioning of the tubes at the mid-length cross section (**Figure 6c**) and manual measurement using a calibrated micrometer.

Using the optimization software and the settings defined in **Table 2**, 100 simulations (10 iterations of 10 runs) for the 0.9 mm thick tube and 60 simulations (6 iterations of 10 runs) for the 1.2 mm thick tube were required to find their respective optimum load paths, as illustrated in **Figure 7**. For comparison purposes, the free-end load path for each tube thickness is also given in **Figure 7**.

© 2015 Government of Canada

Can. Aeronaut. Space J. Downloaded from pubs.casi.ca by April Duffy on 07/14/15
For personal use only.

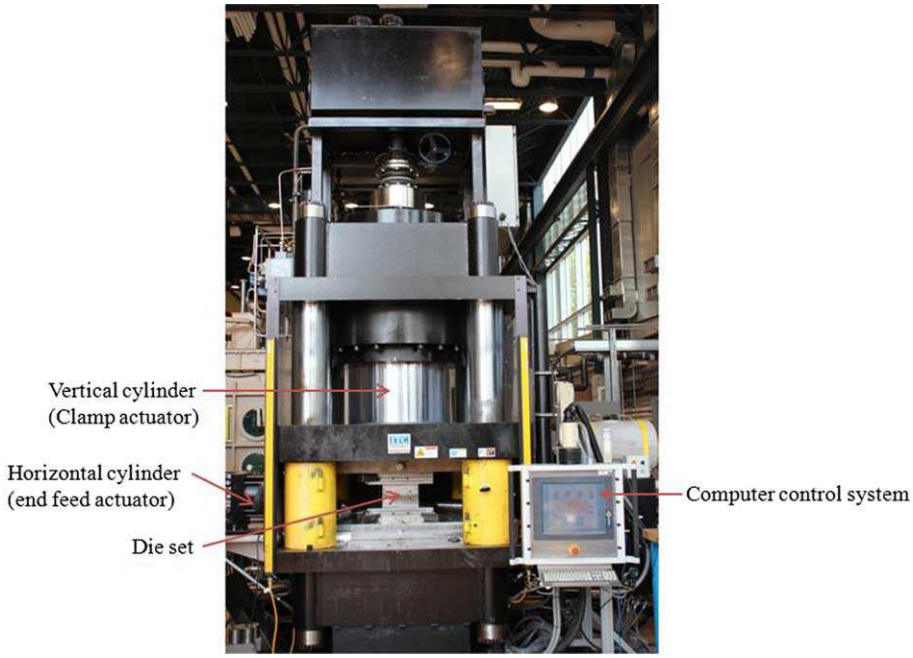

Figure 4. Hydroforming press at NRC.

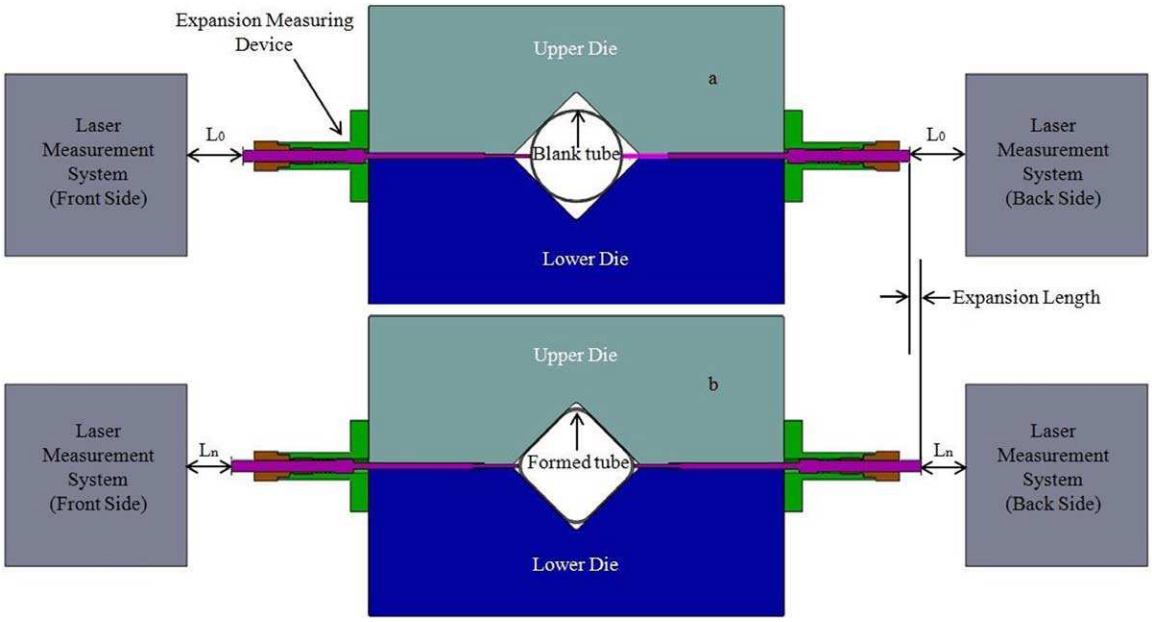

Figure 5. Expansion measurement unit at (a) initial stage and (b) final stage.

Thickness distribution

For each tube thickness, the evolution of the thickness at the mid-length obtained from the simulations was compared with the measured values from the THF experimental results (**Figure 8**). From this figure, it can be observed that maximum thinning occurs close to the corner of the square cross section at the end of the contact region between the tube and the die. Here, the tube is subjected to a tensile stress in the circumferential direction, as it cannot slide further along the die due to the high friction forces in this region. From **Figure 8**, it can also be seen that the thinning pattern is similar for both tube thicknesses. These findings suggest that the optimum load path results in a more uniform thickness distribution as the respective optimum

 © 2015 Government of Canada

Can. Aeronaut. Space J. Downloaded from pubs.casi.ca by April Duffy on 07/14/15
For personal use only.

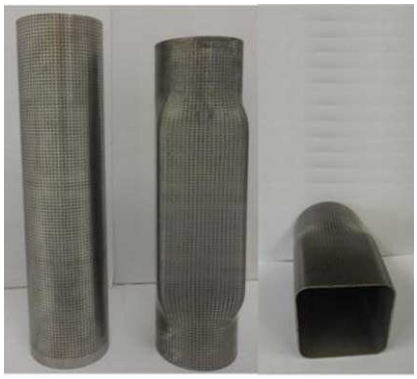

Figure 6. (a) Initial tube, (b) hydroformed tube, and (c) mid-length cross section of the tube.

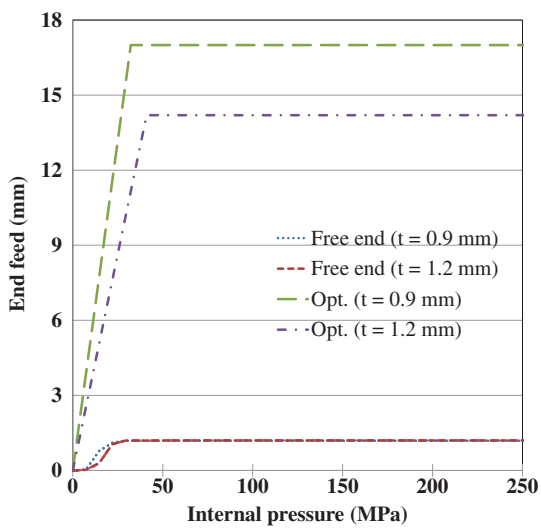

Figure 7. Free-end and optimum load paths for 0.9 mm and 1.2 mm thick tubes.

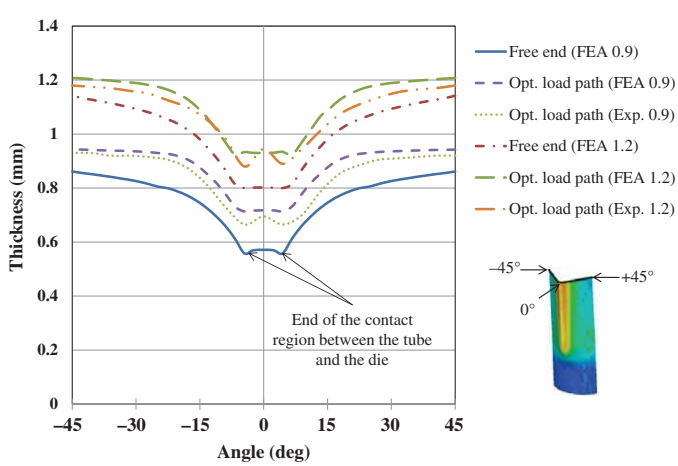

Figure 8. Thickness distributions in the 0.9 mm and 1.2 mm thick tubes with different load paths.

Table 3. Load paths applied to the 0.9 mm and 1.2 mm thick SS321 tubes.

	Optimized pressure (MPa)	End feed (mm)	Minimum thickness (mm)
Free-end (0.9 mm)	—	1.2	0.56
Optimum (0.9 mm)	32.2	17.0	0.72
Free-end (1.2 mm)	—	1.2	0.80
Optimum (1.2 mm)	41.0	14.2	0.96

curve shows smaller "peaks" at the end of the contact region. This is mainly due to the fact that the end feeding pushes more material into the deformation zone, which renders a more uniform thickness distribution. As revealed in **Figure 8**, the simulations results allow prediction of the tube thickness distribution in the 0.9 mm and 1.2 mm thick SS321 tubes with good accuracy (less than 4%).

Table 3 summarises the applied load path and the minimum thickness measured for both tube thicknesses. For the optimum load path, the minimum thickness obtained for each tube thickness was closer to the original thickness values (i.e., 0.9 mm and 1.2 mm). Specifically, as compared with the free-end load path, the thickness at the mid-length was higher for the optimum load path by 28% and 20% for the 0.9 mm and 1.2 mm thick SS321 tubes, respectively. This confirms the validity of the optimization process for determining the optimum load path for THF with the objective of increasing the uniformity in the tube thickness.

Tube expansion

Figure 9 illustrates the tube expansion as a function of the internal pressure for both tube thicknesses. For THF of SS321, tube expansion with the optimum load path was greater than the free-end load path up to an internal pressure of 50 MPa, which indicates that an increased end feed resulted in a higher tube expansion at the beginning of the process. At 50 MPa, end feeding during TFH was stopped and tube expansion continued with increasing internal pressure. Although the final tube expansion values in **Figure 9** are comparable between the free-end and optimum load paths, the higher end feeding with the latter resulted in a lower thickness reduction, as described above. Specifically, the increased thickness of both tubes with the optimum load path increases the resistance to plastic deformation at the corners, which explains the reduced expansion after 50 MPa. For instance, the maximum tube expansions obtained from the simulation and experiments using the optimum load path are equal to 8.34 mm and 8.7 mm for the 0.9 mm thick tubes and 8.09 mm and 8.48 mm for the 1.2 mm thick tubes, respectively. This indicates an error of less than 5% between the FEA and experimental results for both SS321 tubes. In addition, as revealed in

© 2015 Government of Canada

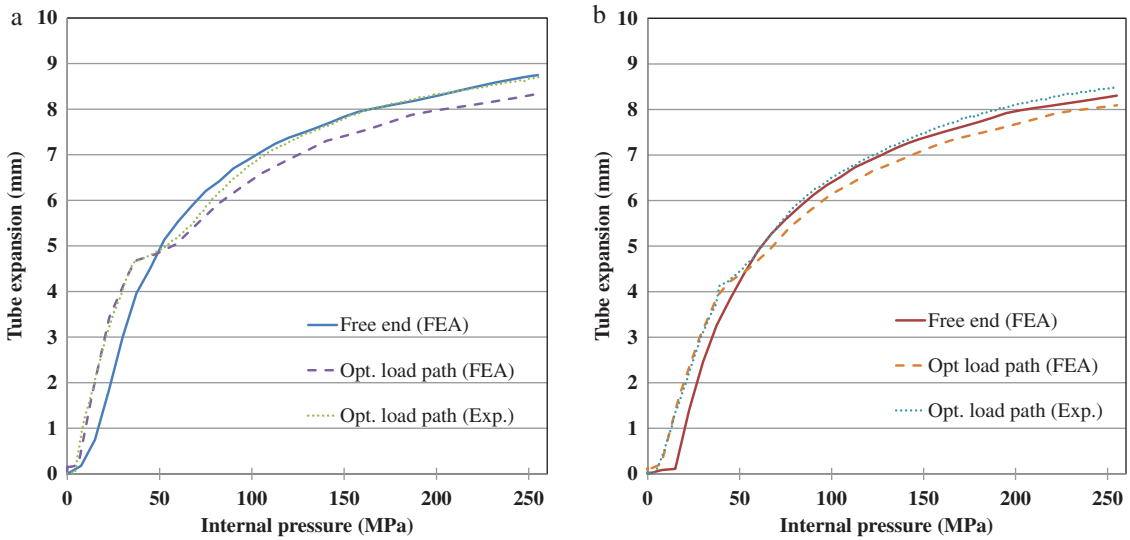

Figure 9. Tube expansion curves for (a) 0.9 mm and (b) 1.2 mm thick tubes.

Can. Aeronaut. Space J. Downloaded from pubs.casi.ca by April Duffy on 07/14/15
For personal use only.

Figure 9, the simulation results for both tube thicknesses predict the same trend and are in good agreement with the experimental results from THF.

Conclusion

For a round-to-square tube hydroforming (THF) process, an optimized load path was obtained through an optimization procedure embedded in commercially available software. Using the optimum load path for THF of SS321 led to greater uniformity in the tube thickness distribution. Compared with the free-end load paths, the optimum load paths increased the minimum tube thickness by 28% and 20% for 0.9 mm and 1.2 mm thick tubes, respectively, and maximum thinning occurred at the end of the contact region of the tube and the die. Also, tube expansion with the optimum load path was higher than the free-end load path up to an internal pressure of 50 MPa, at which point end feeding was stopped. The maximum error between the simulation results and the experimental data for the tube expansion using the optimum load path was less than 5% for both tube thicknesses. It is noteworthy that the predicted results could have shown a better match with the experimental data if a higher order element and the effect of anisotropy and springback were considered in the FEM simulation. These will be considered in our future work on THF.

Acknowledgments

The authors would like to extend their gratitude for the funding received for this project from the Natural Sciences and Engineering Research Council of Canada (NSERC) and the Consortium for Research and Innovation in Aerospace in Quebec (CRIAQ). The authors are also grateful to Maxime Guérin for his support in performing the THF experiments.

References

Abedrabbo, N., Zafar, N., Averill, R., Pourboghrat, F., and R. Sidhu. 2011. Optimization of a Tube Hydroforming Process. In SME Technical Papers – 3rd and 4th Quarter 2011. (One SME Drive – P.O. Box 930, Dearborn, 48121-0930, United States) vol. TP11PUB20, p. 1–6. Coll. Technical Paper-Society of Manufacturing Engineers: Society of Manufacturing Engineers.

Alaswad, A., Olabi, A.G., and Benyounis, K.Y. 2010. A Comparison between RSM and Classical Iterative Optimization Algorithms for Bi-layered Tube Hydroforming. In Proceedings IMC27 Conference, *Galway Mayo Institute of Technology, Ireland, 1st-3rd September*, pp. 185–192.

An, H. 2010. Multi-objective Optimization of Tube Hydroforming Using Hybrid Global and Local Search. Ph.D. thesis, University of Windsor, Canada, 218 p. In ProQuest Dissertations & Theses Full Text.

Aydemir, A., de Vree, J.H.P., Brekelmans, W.A.M., Geers, M.G.D., Sillekens, W.H., and Werkhoven, R.J. 2005. An Adaptive Simulation Approach Designed for Tube Hydroforming Processes. *Journal of Materials Processing Technology*, Vol. 159, No. 3, pp. 303–310. doi: 10.1016/j.jmatprotec.2004.05.018.

Endelt, B., and Nielsen, K. 2001. Least-square Formulation of the Object Function, Applied on Hydro Mechanical Tube Forming. In *Sheet Metal 2001, Proceedings of the 9th International Conference*. ed. / Duflou, Geiger, Kals, Shirvani, Singh. 2–4 March 2001, Leuven, Belgium.

Fann, K.-J., and Hsiao, P.-Y. 2003. Optimization of Loading Conditions for Tube Hydroforming. *Journal of Materials Processing Technology*, Vol. 140, No. 1–3, pp. 520–524. doi: 10.1016/S0924-0136(03)00778-7.

Farimani, S.M., Champliaud, H., Gholipour, J., Savoie, J., and Wanjara, P. 2013. Numerical and Experimental Study of Tube Hydroforming for Aerospace Applications. *Key Engineering Materials*, Vol. 554–557, pp. 1779–1786. doi: 10.4028/www.scientific.net/KEM.554-557.1779.

© 2015 Government of Canada

Can. Aeronaut. Space J. Downloaded from pubs.casi.ca by April Duffy on 07/14/15
For personal use only.

Gholipour, J., Worswick, M., and Oliveira, D. 2004. Application of Damage Models in Bending and Hydroforming of Aluminum Alloy Tube. SAE Technical Paper 2004-01-0835.

Hama, T., Ohkubo, T., Kurisu, K., Fujimoto, H., and Takuda, H. 2006. Formability of Tube Hydroforming Under Various Loading Paths. *Journal of Materials Processing Technology*, Vol. 177, No. 1–3, pp. 676–679. doi: 10.1016/j.jmatprotec.2006.03.213.

Hwang, Y.M., Lin, Y.K., and Chuang, H.C. 2009. Forming Limit Diagrams of Tubular Materials by Bulge Tests. *Journal of Materials Processing Technology*, Vol. 209, pp. 5024–5034.

Jansson, M., Nilsson, L., and Simonsson, K. 2007. On Process Parameter Estimation for the Tube Hydroforming Process. *Journal of Materials Processing Technology*, Vol. 190, No. 1–3, pp. 1–11. doi: 10.1016/j.jmatprotec.2007.02.050.

Jirathearanat, S., and Altan, T. 2004. Optimization of Loading Paths for Tube Hydroforming. In Materials Processing and Design. Modeling, Simulation and Applications. NUMIFORM 2004. *Proceedings of the 8th International Conference on Numerical Methods in Industrial Forming Processes*, 13–17 June 2004, Ohio State University, Columbus, Ohio. pp. 712, 1148–1153.

Johnson, K.I., Nguyen, B.N., Davies, R.W., Grant, G.J., and Khaleel, M.A. 2004. A Numerical Process Control Method for Circular-tube Hydroforming Prediction. *International Journal of Plasticity*, Vol. 20, No. 6, pp. 1111–1137. doi: 10.1016/j.ijplas.2003.10.006.

Koç, M., Allen, T., Jiratheranat, S., and Altan, T. 2000. The Use of FEA and Design of Experiments to Establish Design Guidelines for Simple Hydroformed Parts. *International Journal of Machine Tools and Manufacture*, Vol. 40, No. 15, pp. 2249–2266. doi: 10.1016/S0890-6955(00)00047-X.

Labergere, C., and Gelin, J.C. 2004. New Strategies for Optimal Control of Command Laws for Tube Hydroforming Processes. In Materials Processing and Design. Modeling, Simulation and Applications. NUMIFORM 2004. *Proceedings of the 8th International Conference on Numerical Methods in Industrial Forming Processes*, 13–17 June, Ohio State University, Columbus, Ohio. pp. 712–1141.

LS-Dyna Keyword User's Manual. 2013. Version 971, Livermore Software Technology Corporation (LSTC), USA, February.

LS-OPT User Manual. In *A Design Optimization and Probabilistic Analysis Tool for the Engineering Analyst, Version 4.2*, Livermore Software Technology Corporation.

Mataei, M., Gakwaya, A., Guillot, M., and Lévesque, J. 2011. Virtual Modeling of Tube Hydroforming Process of Complex Aluminum Parts. In *Conference of Metallurgists*, CIMMM, Montreal, Canada, p. 350.

Meinders, T., Burchitz, I.A., Bonte, M.H.A., and Lingbeek, R.A. 2008. Numerical Product Design: Springback Prediction, Compensation and Optimization. *International Journal of Machine Tools and Manufacture*, Vol. 48, No. 5, pp. 499–514. doi: 10.1016/j.ijmachtools.2007.08.006.

Ray, P., and MacDonald, B.J. 2004. Determination of the Optimal Load Path for Tube Hydroforming Processes Using a Fuzzy Load Control Algorithm and Finite Element Analysis. *Finite Elements in Analysis and Design*, Vol. 41, No. 2, pp. 173–192. doi: 10.1016/j.finel.2004.03.005.

Ray, P., and MacDonald, B.J. 2005. Experimental Study and Finite Element Analysis of Simple X- and T-branch Tube Hydroforming Processes. *International Journal of Mechanical Sciences*, Vol. 47, No. 10, pp. 1498–1518. doi: 10.1016/j.ijmecsci.2005.06.007.

Saboori, M., Champliaud, H., Gholipour, J., Gakwaya, A., Savoie, J., and Wanjara, P. 2014. Evaluating the Flow Stress of Aerospace Alloys for Tube Hydroforming Process by Free Expansion Testing. *The International Journal of Advanced Manufacturing Technology*, Vol. 72, No. 9–12, pp. 1275–1286. doi: 10.1007/s00170-014-5670-5.

Sillekens, W., and Werkhoven, R. 2001. Hydroforming Processes for Tubular Parts: Optimisation by Means of Adaptive and Iterative FEM Simulation. *International Journal of Forming Processes*, vol. 4, No. 3–4, pp. 377–393. doi: 10.3166/ijfp.4.377-393.

Yang, J.-B., Jeon, B.-H., and Oh, S.-I. 2001. Design Sensitivity Analysis and Optimization of the Hydroforming Process. *Journal of Materials Processing Technology*, Vol. 113, No. 1–3, pp. 666–672. doi: 10.1016/S0924-0136(01)00670-7.

© 2015 Government of Canada